Sensors and Actuators B 145 (2010) 575–582

Contents lists available at ScienceDirect

Sensors and Actuators B: Chemical

journal homepage: www.elsevier.com/locate/snb

Surface modification of nano-porous anodic alumina membranes and its use in electroosmotic flow

Yu-Feng Chen[a,*], Yi-Hsin Hu[b], Yen-I Chou[a], Shih-Ming Lai[b], Chi-Chuan Wang[c]

[a] Energy and Environment Research Laboratories, Industrial Technology Research Institute, 310 Hsinchu, Taiwan
[b] Department of Chemical and Materials Engineering, National Yunlin University of Science and Technology, Yunlin, Taiwan
[c] Department of Mechanical Engineering, National Chiao Tung University, 300 Hsinchu, Taiwan

ARTICLE INFO

Article history:
Received 10 July 2009
Received in revised form 5 November 2009
Accepted 27 December 2009
Available online 4 January 2010

Keywords:
Electroosmotic pump
Surface modification
Zeta potential
Porous anodic aluminum membrane

ABSTRACT

This study examines the surface-modification effects of porous anodic alumina membranes (PAAMs) on the performance of electroosmotic (EO) pumping. The modifications include using H_2O_2-pretreated, and followed by 3-aminopropyltriethoxysilane (APS) or 3-mercaptopropyl trimethoxysilane (MPTS) sol–gel solutions to functionalize the surface of PAAM for achieving higher surface charge density. The surface-modified membranes are analyzed by average pore size, contact angle, and FTIR measurements. The results show that APS and MPTS are successfully coated on the surface of PAAMs. The characteristics (e.g., total current, maximum pressure, and normalized flow rate) of the EO pumps with these surface-modified PAAMs are investigated. The comparison results of total current at zero time confirmed that the surface charge density of the surface-modified PAAM has been increased. Consequently, the maximum normalized flow rate of EO pump with the APS- and MPTS-coated PAAM are higher than that with the bare PAAM in DI water but without buffer control methods. The convection current of EO flow is also investigated, and the results show that its contribution to total current is around 11% and thus cannot be ignored for EO flow with nano-size channels.

1. Introduction

Electroosmotic (EO) pumps, featuring no moving parts and making use of the electroosmosis principle to direct fluid flow, had been successfully implemented in various micro/nano-electromechanical systems (MEMS/NEMS) [1] such as micro-electronic cooling [2] and biomedical analysis [3]. Most of the conventional EO pumps were fabricated by packing silica microspheres or polymeric porous frits as the capillary channels [4–6]. These porous capillary channels had poor uniformity in pore size and high tortuosity, and therefore often entail sufficiently high voltage (from hundreds to a few kV) to compensate these inherited limitation. For example, supplied voltages of 2, 1, and 6 kV were respectively reported by Zeng et al. [4], Reichmuth et al. [5], and Wang et al. [6]. But a high application voltage makes EO pumps extremely difficult to be integrated into a NEMS/MEMS. Hence, it would be very helpful to reduce the working voltage of EO pumps while still retain their performance. One common way was via modifying surface morphology to lower the working voltage. Several researches [7–11] had successfully used porous membranes with high porosity, low tortuosity, uniform pore size and short channel length to reduce the operation voltage (<100 V) while still keep the pumping performance. Two of the commonly used porous membranes were made from silicon-dioxide and anodic alumina. Yao et al. [7] demonstrated an EO pump with a porous silicon membrane is capable of achieving a maximum flow rate of 3.2 ml/min at just 25 V. However, the buffer control method is needed to achieve this flow rate. This is due to the silicon membrane only can achieve a maximum average zeta potential (around −104 mV) at the working fluid with pH ∼ 9.

It is noticed that alumina is an amphoteric material with surface electrical properties depending on the pH value of working fluid. Its isoelectric point is at a pH value around 8 [8]. When the pH value of working fluid is less than 8, alumina is protonated to become positively charged surface. By contrast, it becomes a negatively charged surface when the pH value is above 8. Earlier studies [8–11] had reported the EO pump with a porous anodic alumina membrane (PAAM). Vajandar et al. [9] reported an EO pump with a thin layer of SiO_2 coated on PAAM could achieve a flow rate higher than that with a bare PAAM at a solution of pH ∼ 9. The reason was that, in a solution of pH ∼ 9, the zeta potential of bare PAAM is only around 15–35 mV [9] which is well below the zeta potential of SiO_2-coated PAAM (∼−104 mV). Generally, the zeta potential of aluminum oxide is reported to be approximately

* Corresponding author at: 409C, Bldg. 64, 195, Section 4, Chung Hsing Rd., Chutung, 310 Hsinchu, Taiwan. Tel.: +886 3 5915376; fax: +886 3 5820250.
E-mail addresses: JoanChen@itri.org.tw, yubau_chen@yahoo.com.tw (Y.-F. Chen).

0925-4005/$ – see front matter © 2009 Elsevier B.V. All rights reserved.
doi:10.1016/j.snb.2009.12.061

80 mV at a solution of pH ~ 6.5 [12,13]. Chen et al. reported [10] an EO pump with a bare PAAM in DI water (pH ~ 6.2) (without buffer control methods) could achieve a normalized flow rate as high as 0.09 mL min^{-1} V^{-1} cm^{-2}. It is apparent that the EO pump with a bare PAAM can be operated in low ionic electrolyte or DI water without buffer control methods. It is potentially suitable for many applications, such as microelectronic cooling systems.

The techniques of surface modification are commonly used to improve hydrophilicity, to introduce reactive functional groups, and to immobilize functional protein molecules of surface [14]. To authors' knowledge, Miao et al. [11] was the first group to increase the EO pump flow rate via treating the PAAM surface by some strong oxidants (H_2O_2 and $H_2SO_4/Na_2Cr_2O_7$). The surface treatments had considerably increased the oxygen vacancies on the PAAM surface and consequently lowered the working voltage. It is the objective of this study to provide some alternative surface modification methods onto PAAM surface for enhancing EO pumping performance without buffer control methods. Hydrogen peroxide (H_2O_2) pretreatment and followed by 3-aminopropyltriethoxysilane (APS), or 3-mercaptopropyl trimethoxysilane (MPTS) functionalization are chosen as the surface modification methods on PAAM to manipulate its surface charge. The characteristics of PAAM are examined by using average pore size, contact angle and FTIR measurements. The characteristics of the EO pumps with these surface-modified PAAMs are investigated by comparing their total currents, maximum pressures, and normalized flow rates.

2. Theoretical model

The electrical properties of PAAM surfaces depend on the pH value of solution. The pH value of the present working fluid (DI water) is near 6.2, thus the surface of PAAM is protonated and positively charged [8].

$$\text{Al–OH} + \text{H}^+ \rightarrow \text{Al–OH}_2^+ \tag{1}$$

When a voltage is applied across an alumina membrane, the excess counterions (OH^- of DI water) repelled from the electric double layer (EDL) of the nano-pore will carry the liquid molecules alongside by viscous force, the induced flow is so called an electroosmotic flow (EOF). For further increasing the flow rate, this study adopts the porous alumina membrane for it offers high porosity, low tortuosity, and thin channel length, which are the key factors of the present EO pump [9–11]. With the low tortuosity, each of the pores of the alumina membrane can be considered as an independent cylindrical channel. The detailed electroosmotic flow model is presented as follow.

2.1. Electroosmotic flow model

The electroosmotic flow through a cylindrical pore can be expressed as [15]

$$u(r) = -\frac{1}{4\eta}(a^2 - r^2)\frac{dp}{dx} - \frac{\varepsilon}{4\pi\eta}[\zeta - \psi(r)]E \tag{2}$$

where dp/dx is the pressure gradient, a is the radius of circular tube, r is the distance from symmetry axial, η is the viscosity, ε is the permittivity of the electrolyte, ζ is the zeta potential, $\psi(r)$ is the radial potential due to the electric double layer, E is the strength of the electric field, respectively.

The volume flow rate (Q) is given by [15]

$$Q = 2\pi\int_0^a ru(r)\,dr = -\frac{\pi a^4}{8\eta}\frac{\Delta P}{L} - \frac{\varepsilon\zeta a^2(1-G)E}{4\eta} \tag{3}$$

where ΔP is the pressure difference across the channel, L is the corresponding channel length and G is the ratio of the mean electrostatic potential across the capillary to the ζ-potential, respectively. G in Eq. (3) is represented as

$$G = \frac{2}{\zeta a^2}\int_0^a r\psi(r)\,dr \tag{4}$$

where $\psi(r)$ is the potential. In a symmetric electrolyte solution, $z^+ = -z^-$, the Poisson–Boltzmann (PB) equation can be employed

$$\frac{1}{r}\frac{d}{dr}\left(r\frac{d\psi}{dr}\right) = \frac{2n_0 ze}{\varepsilon}\sinh\left(\frac{ze\psi}{kT}\right) \tag{5}$$

where n_0 is the ionic number concentration, z is the absolute value of the ionic valence, e is the fundamental charge of an electron, k is the Boltzmann constant, and T is the absolute temperature, respectively.

2.2. Maximum volume flow rate of EO pump

The maximum volume flow rate (Q_{max}) can be evaluated directly from Eq. (3) by setting the pressure difference (ΔP) to zero. The maximum volume flow rate generated by electroosmosis flow can be expressed as

$$Q_{max} = -\frac{\varepsilon\zeta a^2(1-G)E}{4\eta} \tag{6}$$

By contrast, with a given maximum pressure difference (ΔP_{max}), it then corresponds to the zero net volume flow rate condition ($Q = 0$) from Eq. (3). From Eq. (6), with a given membrane geometry (e.g., pore size, porosity, and tortuosity) and working fluid, and maintaining an electrical field, Q_{max} is proportional to the zeta potential (ζ). Denoting the zeta potential of surface coated PAAM as ζ_{coated} and the zeta potential of bare PAAM as ζ_{bare}, thus the ratio of maximum volume flow rate of EO pump with a coated PAAM to EO pump with a bare PAAM can be expressed as

$$\frac{Q_{max,coated}}{Q_{max,bare}} \approx \frac{\zeta_{coated}}{\zeta_{bare}} \tag{7}$$

From Eq. (7), the maximum volume flow rate of an EO pump can be increased by raising the zeta potential (or surface charge) of PAAM.

2.3. Total current of EO pump

The ionic current, I, of electroosmotic flow in a single cylindrical channel is the summation of the conductive current (I_{cond}) and convective current (I_{conv}) contributions [16]

$$I = 2\pi e\left\{\int_0^a [(n_- + n_+)\mu E]rdr + \int_0^a [(n_- - n_+)u(r)]rdr\right\} \tag{8}$$

where e is the electron charge, n_+ and n_- are the density of positive and negative ions, μ is the ion mobility, and E is the parallel electric field which is calculated by an applied voltage V divided by the channel length L, respectively. The positive (H^+) and negative (OH^-) ion mobility are assumed identical. The average pore size of present PAAM is near 200 nm. The working fluid is DI water which gives a low ionic concentration ~10^{-7} M. Thus, the thickness of EDL is approximately 960 nm, which is larger than the pore size (200 nm) of PAAM used in present study. Therefore, the surface charges dominate the ion transport in the nano-pore of PAAM [16,17].

In the regime of low electrolyte concentration, the surface charge density (σ) will govern the ionic concentration inside the channel to maintain electroneutrality [17]. In a solution of pH ~ 6.2, PAAM is positively charged so that the counterions (OH^-) accumulate near the charged surface while the co-ions (H^+) are electrostatically repelled. The density of counterions (OH^-) inside

the nano-pore is expressed as $n_{-} = \sigma/2\pi ea$ which is then substituted into the first term of RHS of Eq. (8). σ is the surface charges density. The conduction current can be expressed as

$$I_{\text{cond}} = 2\pi e \int_0^a \frac{\sigma}{2\pi ea} \mu E r dr = \frac{1}{2}\sigma \mu E a \tag{9}$$

From Eq. (9), the conduction current is proportional to the surface charge density, σ. Hence the total current of the present EO pump is derived from the surface charge density of coated PAAM. Despite the flow rate is proportional to the zeta potential as appeared in Eq. (7), it must be emphasized that the zeta potential ζ is the potential between the stern layer and electrical double layer. Therefore the zeta potential is actually proportional to the surface charge density, i.e. $\zeta \propto \sigma$.

3. Experimental verification

3.1. Materials

The PAAMs (purchased from Whatmann Inc.) used in this study have a nominal pore size of 200 nm, a pore density of 10^9 per cm^2, a diameter of 2.1 cm, and a thickness of 60 μm, respectively. The surface modification methods include hydrogen peroxide (30% H_2O_2, Sigma–Aldrich) pretreatment, and followed by 3-aminopropyltriethoxysilane (APS, NH_2–$(CH_2)_3$–$Si(OCH_3)_3$) (95%, Aldrich), or 3-mercaptopropyl trimethoxysilane (MPTS, $HS(CH_2)_3Si(OCH_3)_3$) (95% MPTS, Aldrich) immobilization for more surface charge density (zeta potential). The values of pK_a for the aminopropyl group (–R–NH_2) in APS and for the thiolate group (–R–SH) in MPTS are 10.7 [18] and 10.0 [19], respectively. The working fluid used in this study is deionized (DI) water. Acetone (99.7% purity) was purchased from Baker used directly without further purification.

3.2. Membrane preparation

3.2.1. H_2O_2-pretreated process

A bare PAAM was dipped in H_2O_2 aqueous solution with a volume concentration of 30% for 2 h, and subsequently cleaned by DI water. After then, the membrane was placed in an oven controlled at 100 °C and 26 cm-Hg for over 6 h. The hydroxyl-group (–OH) on the PAAM surface is expected to rise after the above H_2O_2-pretreated process.

3.2.2. APS-coated process

The schematic of silanization process of APS-coated on PAAM is shown in Fig. 1a. APS spontaneously reacted with surface hydroxyl-group and it formed a self-assembled layer. After the H_2O_2-pretreated process as described at Section 3.2.1, the PAAM was immersed in an APS/acetone solution with a volume fraction of 1:100 for 3 h, and then rinsed by acetone. Subsequently, the APS-coated PAAM was also placed in an oven controlled at 100 °C and 26 cm-Hg for over 24 h [20,21].

3.2.3. MPTS-coated process

The schematic of silanization and subsequent oxidation process for MPTS-coated is shown in Fig. 1b. For simplification, we will use "MPTS-coated" to represent the whole process of the MPTS silanization step and the subsequent oxidation step in the following discussion. After the H_2O_2-pretreated process as described in Section 3.2.1, the PAAM was dipped in an MPTS/acetone solution with a volume fraction of 1:100 for 3 h, and then rinsed by acetone. Then, the PAAM was baked at a temperature of 100 °C and at a system pressure of 26 cm-Hg for over 12 h. The above process is called as the MPTS silanization step. Then this membrane was immersed in 30% H_2O_2 aqueous solution for over 1 day for oxidation, and then dried by nitrogen. This process is called as the oxidation step, which transfers the end functional group of MPTS from –SH to $-SO_3H$ (Fig. 1b).

3.3. Membrane characterizations

3.3.1. Pore size measurement

The schematic of the average pore size measurement system is shown in Fig. 2. The average pore radius, a, calculated by using Hagen–Poiseuille law, is expressed as

$$a = \left(\frac{8Q\eta L}{\pi \Delta P A n_p} \right)^{1/4} \tag{10}$$

where Q is the volume flow rate, ΔP is the pressure difference, L is the thickness of membrane, n_p is the pore density ($10^9/cm^2$), and A

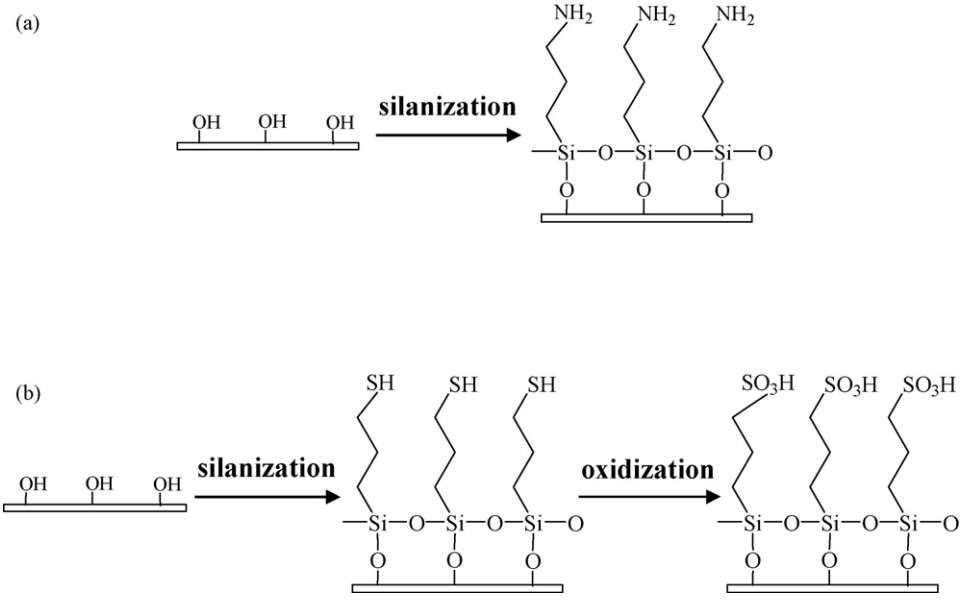

Fig. 1. The mechanisms of (a) APS-coated process, and (b) MPTS-coated process on PAAM surface.

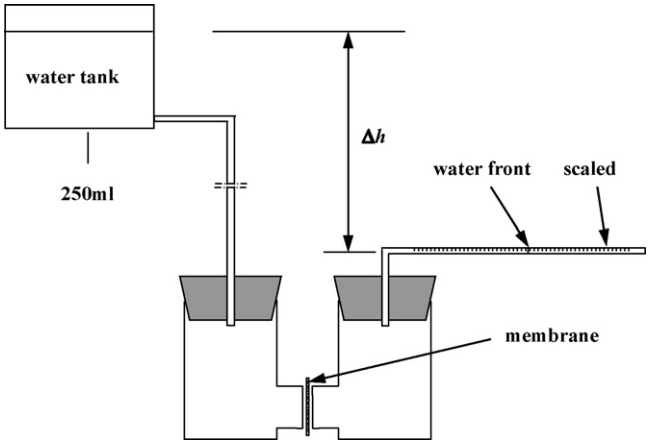

Fig. 2. The schematic of the membrane average pore size measurement system.

is the total surface area of membrane, respectively. The ΔP is calculated from $\rho g \Delta h$. Where Δh is the high difference between two reservoirs (shown in Fig. 2), ρ is the density, and g is the acceleration of gravity, respectively. The accumulated flow volume for a given Δh is recorded with time by using a precision weighting balance (AND GF300). The volume flow rate Q is calculated as the accumulated flow volume divided by the period of elapsed time. The measurement uncertainty of accumulated flow volume and Δh are ± 0.001 g and ± 0.1 mm.

3.3.2. Contact angle measurement

The contact angle measurement (DSA100, KRUSS) was used to distinguish the degree of hydrophilicity among the bare PAAM and the PAAMs coated with different molecules. DI water was used as the working fluid.

3.3.3. FTIR measurement

The attenuated total reflection-Fourier transfer infrared (ATR-FTIR, PerkinElmer Spectrum 1) was employed to examine the existence of APS or MPTS molecules on PAAMs. The FTIR absorption spectrum of pure compound was measured by mixing it with KBr at a ratio of 1:4 (w/w). The coated membrane was fixed on the holder of ATR and the transmittance spectrum was measured. The spectrum was scanned from 700 to 4000 cm^{-1} with DPI and scan rate being set to 4.0 cm^{-1} and 128 s, respectively.

3.4. EO pump experimental setup

The schematic of experimental setup to examine the performance of EO pump is shown in Fig. 3 [10]. The fluidic system includes a holder which contains a bare PAAM or the PAAM with surface modification, a pair of Pt mesh electrodes, and a pair of Pt wire electrodes. The nano-porous alumina membrane, perpendicular to the flow direction, is placed between a pair of Pt mesh electrodes. The SEM images of PAA membrane is also shown in Fig. 3. The fluid within the channel is driven by an applied electric field (power supplier, GW Instek GPR-11H30D). The resultant flow rate and current are measured by an electronic balance meter (AND GF300) and a multi-sourcemeter (Keithley 2400), respectively.

The DI water used in the present experiment is generated by Synergy 185 UV Ultrapure Water System (purchased from Millipore Company). Its pH value is around 7.2 rights out of the generator, drops to around 6.2 after 25 min, and keeps stable after then. To ensure a stable pH value, the DI water as used in each test is first put in a vessel for more than 30 min.

Detailed manufacturing process of Pt mesh electrodes was described in an earlier publication [10] and is not repeated here.

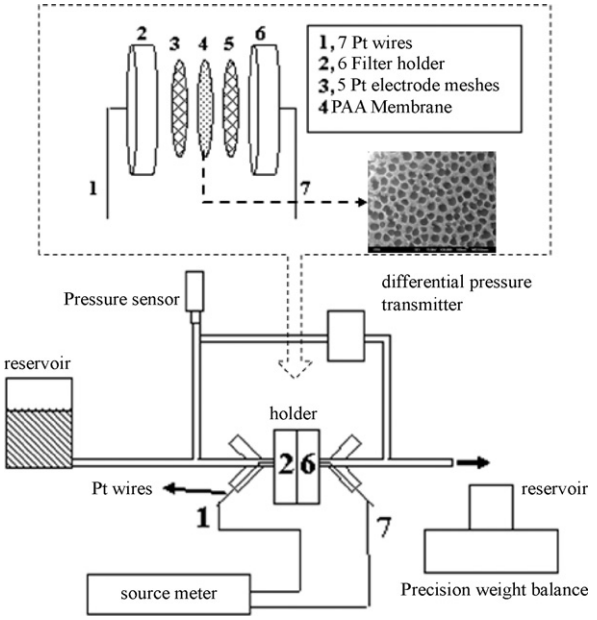

Fig. 3. Schematic diagram of the EO pump apparatus and the components inside the filter holder, which includes a pair of Pt electrode wires (1,7), a pair of Pt electrode meshes (3,5), and a PAAM (4).

The applied voltage is from 5 to 60 V, and the related electric field is from 8.33×10^4 to 1×10^6 V/m. After applying the electric field, the time history of accumulated flow volume is recorded by a precision weight balance.

4. Results and discussion

4.1. Characteristics of coated membrane

4.1.1. Pore size analysis

Although scanning electron microscopy (SEM, JSM-6500F from JEOL) is used to observe the morphology of PAAM, it is unable to identify the pore size because the coating film on PAAM was too thin. Hagen–Poiseuille law (described in Section 3.3.1) is used to calculate the average pore size of the bare and the surface-modified PAAMs. The measurement errors of volume flow rate (Q) and pressure difference (ΔP) used in Hagen–Poiseuille law are around 0.9% and 0.3%. The calculated average pore diameter of bare PAAM is near 227.2 ± 2.9 nm. After APS- and MPTS-treatments, the calculated average pore diameter are around 226.6 ± 0.9 nm and 225.1 ± 1.1 nm, which are slightly smaller than that of the bare PAAM. According to the above results, the maximum error of present pore size measurement is around 1.3%. These results are in line with some previous studies [22–24]. Kurth and Bein [20] also reported a thickness of APS to be near 0.7 nm while Liu et al. [23] and Xu et al. [24] reported the thickness of MPTS monolayer to be around 0.8 nm.

4.1.2. Contact angle analysis

The contact angles of the bare PAAM, the PAAM with H_2O_2-pretreated, the PAAM with APS-coated, and the PAAM with MPTS-coated are listed in Table 1. The measured contact angle of the bare PAAM is smaller than 5° which is the limitation of present measurement. After the PAAM is pretreated with H_2O_2, the hydroxyl-group on the PAAM surface is increased but the contact angle of the membrane is still less than 5°. When the membrane is further modified by APS, the functional group of PAAM surface is changed from hydroxyl-group to the amino-group (Fig. 1a) and the measured contact angle is increased substantially from 5° to

Table 1
Comparison of the contact angles on the bare PAAM and the PAAM surfaces with H_2O_2-pretreated, APS-coated, and MPTS-coated.

Membrane	Contact angle (degree)
Bare PAAM	<5
H_2O_2-pretreated	<5
APS-coated	53
MPTS-coated	18

53° (Fig. 4a), referring to a hydrophobic behavior. This result is in agreement with Kurth and Bein [22].

In the MPTS-coated process, which includes MPTS silinantion and subsequent oxidation steps, the measured contact angle is first increased from less than 5° to approximately 83° (Fig. 4b) through the MPTS silinantion step and then decreased back to approximately 18° (Fig. 4c) after a subsequent oxidation step. The increase of contact angle is due to the formation of hydrophobic mercapto-group (–SH), and the reduction of contact angle is due to the change of the hydrophobic mercapto-group (–SH) to the hydrophilic sulfonic acid-group ($–SO_3H$). The above changes of contact angle demonstrate that the MPTS was successfully functionalized on the PAAM surface.

4.1.3. FTIR spectra

The ATR-FTIR was employed to examine PAAM. Fig. 5a shows that the FTIR group adsorption regions of the APS-coated PAAM is similar to those of APS compound in KBr. The characteristics peaks include NH_2 bending bands at ~1570 cm^{-1}, asymmetric (υ_a) and symmetric (υ_s) C–H_2 stretching bands at ~2936 and ~2842 cm^{-1}, and Si–O–C stretching band with the stretching of the inorganic Si–O–Si network at 1069 cm^{-1}, respectively. These results indicate that the structure of APS is well implanted on the PAAM surface via silanization process. Fig. 5b shows the FTIR spectra of the MPTS-silanization PAAM, the MPTS-coated PAAM, and MPTS compound in a KBr, respectively. The characteristic peaks of CH_2, Si–O–Si and Si–O–C reveal the same as those appeared in Fig. 5a. After the oxidized process, the MPTS-coated PAAM exhibits the characteristic peaks of SO_2 stretching band at the region of ~1161 cm^{-1} and –OH band at the region of ~1600 and ~3500 cm^{-1}. Based on the findings by Wu et al. [21], –SH groups are transformed to $–SO_3^-H^+$ groups when the PAAM was immersed in H_2O_2 aqueous solution. The SO_2 stretching band indicates that $–SO_3^-H^+$ groups were well functionalized on the PAAM surface and the –OH peak was formed due to the absorption of water on the highly hydrophilic surface of $–SO_3^-H^+$ groups. Therefore, the FTIR spectra indicate that the PAAM surface was well functionalized by MPTS.

4.2. Effects of membrane coating on total current of EO pump

The time histories of accumulated water volume and total current for the EO pumps with bare, H_2O_2-pretreated, APS-coated, and MPTS-coated PAAMs are plotted in Fig. 6. In this test, DI water is used as the working fluid and the supplied voltage is

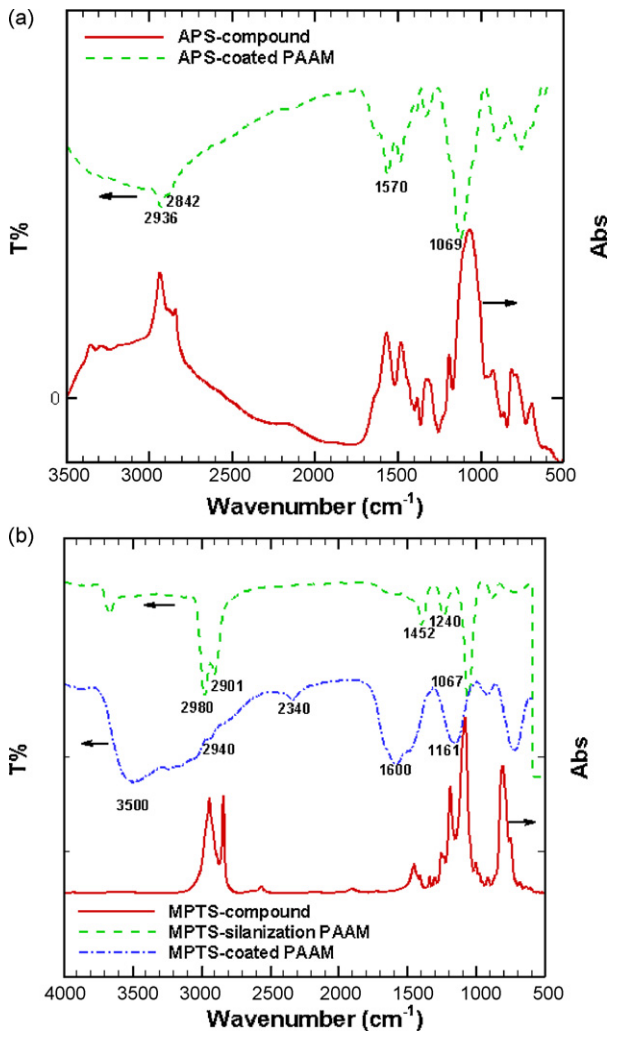

Fig. 5. FTIR spectra of (a) APS compound in KBr and the APS-coated PAAM, and (b) MPTS compound in KBr, the MPTS-silanization PAAM, and the MPTS-coated PAAM.

set to 20 V. At the beginning of experiment, time = 0, there is no convection current from electroosmotic flow. This is due to zero velocity (2nd term of Eq. (8)) and therefore the measured total current is sole conduction current. Our results show that the order of the total current at time = 0, which represents the conduction current only, is $I_{total,APS}$ (1.22 mA) > $I_{total,MPTS}$ (0.75 mA) > I_{total,H_2O_2} (0.74 mA) > $I_{total,bare}$ (0.32 mA). From Eq. (9), the conduction current is proportional to the surface charges density, which reveals that the associated orders of surface charge and zeta potential are $\sigma_{APS} > \sigma_{MPTS} > \sigma_{H_2O_2} > \sigma_{bare}$ and $\zeta_{APS} > \zeta_{MPTS} > \xi_{H_2O_2} > \zeta_{bare}$, respectively. This result has confirmed that the surface charge density of the PAAM has been increased through the H_2O_2-pretreated, the APS- or MPTS-coated process.

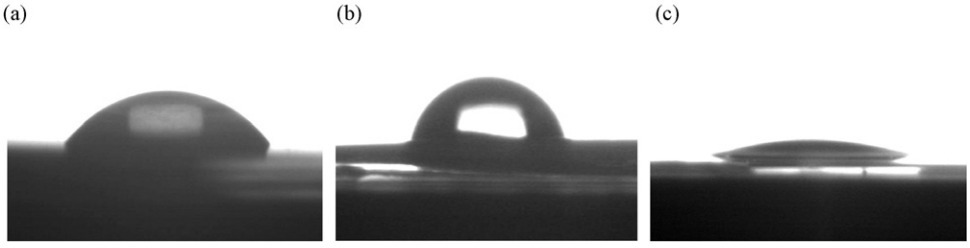

Fig. 4. Water contact angle on the PAAM surface after (a) APS-coated process (53°), (b) MPTS-silanization process (83°), and (c) MPTS-coated process (18°).

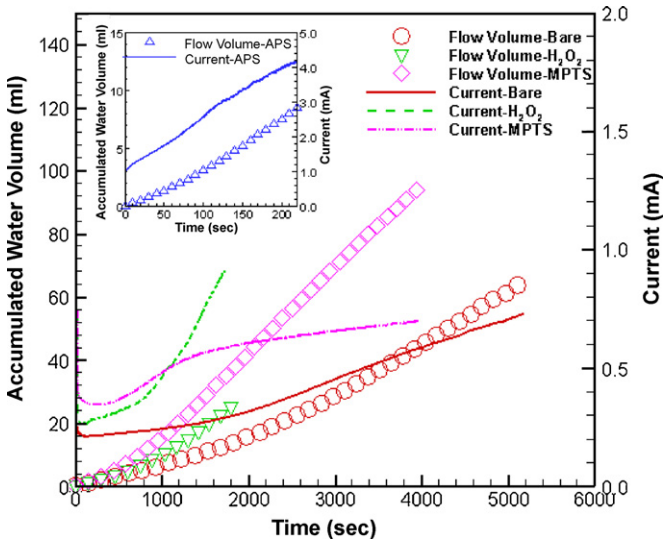

Fig. 6. The time histories of accumulated water volume and total current of the EO pumps with bare, H_2O_2-pretreated, APS-coated, and MPTS-coated PAAMs (DI water, 20 V).

It can also be observed from Fig. 6 that the measured total current of EO pump is increased with elapsed time. This is actually resulted from the convection current of EOF and water electrolysis [25]. Apparently, water electrolysis leads to more H^+ and OH^-, thereby increasing the ionic number of bulk flow. This eventually raises the effective conductivity of bulk flow and then increases the total current accordingly. The result is in line with the previous study [25]. In addition to the above discussion, it is also worthy to mention that the accumulated flow volume is increased linearly with elapsed time, which in turns represents a constant flow rate or velocity before the pump is failed. Although the water electrolysis produces more H^+ and OH^- which causes total current increased linearly with elapsed time, but the number difference between cations and anions in the working fluid is still same. Thus, the number of the excess counterions (OH^- of DI water) of the nano-pore is not changed with time, which causes constant flow rate.

The convection EOF current is further investigated using the EO pump with H_2O_2-pretreated PAAM at 40 V. Fig. 7 shows the time histories of accumulated water volume and total current. At the first stage (time < 135 s), the accumulated water volume and total current are linearly increased with time. Subsequently for 135 s < time < 190 s, the gate valve at the outlet of EO pump is shut

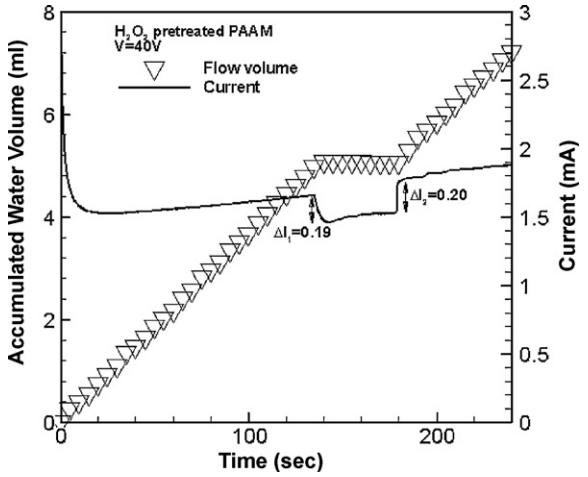

Fig. 7. The time histories of accumulated water volume and total current of the EO pump with H_2O_2-pretreated PAAM (DI water, 40 V).

off, yielding a level-off phenomenon of accumulated volume at this period. At the same time, the total current is significantly dropped from $I = 1.66$ to 1.47 mA ($\Delta I_1 \sim 0.19$ mA). Finally, the outlet valve of EO pump is reopened ($t > 190$ s). Consequently, the total current is raised from 1.53 to 1.73 mA ($\Delta I_2 \sim 0.20$ mA). Through this on-and-off operation, it is found that the contribution of convection current to total current is around 11%. This measured result does not agree with those by Arulanandam and Li [26], who clearly indicated that the convection EOF current was several orders of magnitude lower than the conduction current and it had a negligible contribution to the total current. On the other hand, our result shows the contribution of convection current can be as high as 11%. One possible explanation amid the differences is that the present pore size (0.2 μm) is 500 times smaller than theirs (100 μm). In this regard, overlapping of electrical double layer is much more pronounced in our study, leading to a much higher contribution of convection current.

The data shown in Fig. 6 is recorded before the EO pump is failed. It should be further informed that the lifetime of the EO pump with APS-coated PAAM (Fig. 6) is shorter than others. After the APS-coated process, the PAAM becomes highly brittle, thus reduces the lifetime of EO pump. For the EO pumps with H_2O_2-pretreated, MPTS-coated and bare PAAM, their lifetimes are usually longer than 1 h.

4.3. Effects of membrane coating on EO pump performance

Fig. 8a and b summarize the experimental results of maximum volume flow rate (Q_{max}) and maximum pressure difference

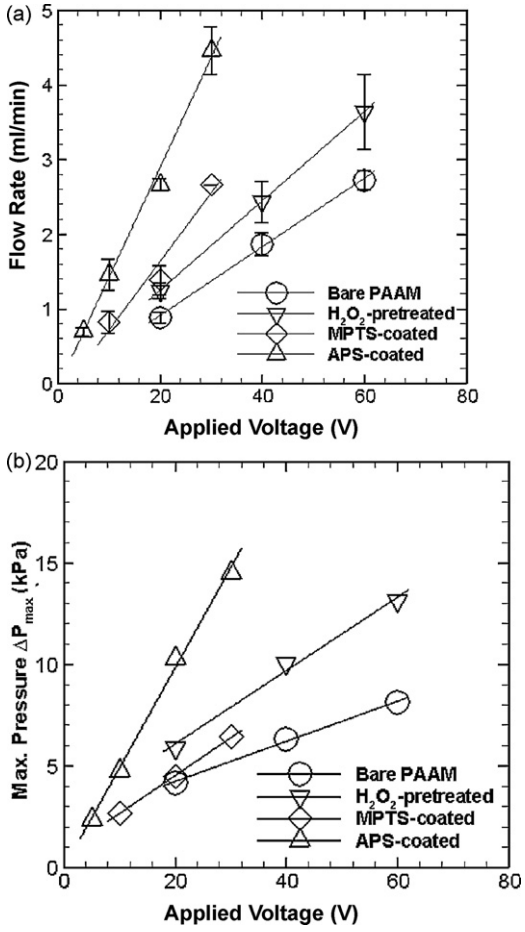

Fig. 8. Effects of applied voltage on (a) maximum volume flow rate, and (b) differential pressure of the EO pumps with bare, H_2O_2-pretreated, APS-coated, and MPTS-coated PAAMs.

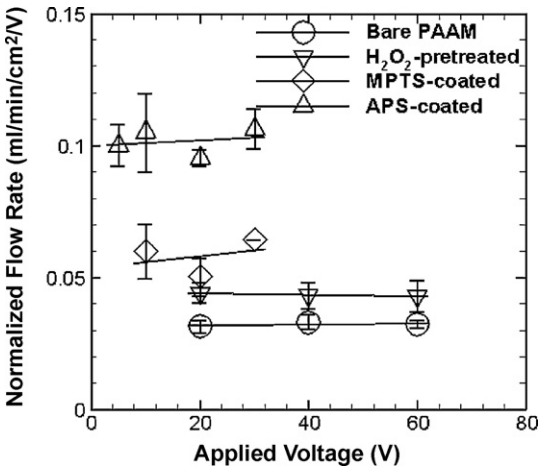

Fig. 9. Comparison of the normalized flow rates on the EO pumps with bare, H_2O_2-pretreated, APS-coated, and MPTS-coated PAAMs.

(ΔP_{max}) of the EO pumps with four kinds of PAAMs. By varying the supplied voltage from 5 to 60 V, the measured Q_{max} and ΔP_{max} are observed to vary linearly against supplied voltage. As derived in Section 4.2, we know that the order of the zeta potential are $\zeta_{APS} > \zeta_{MPTS} > \xi_{H_2O_2} > \zeta_{bare}$. Employing this result along with the estimation from Eq. (7), we can anticipate the maximum volume flow rates of the EO pumps with these four kinds of PAAMs are in the following order: $Q_{APS} > Q_{MPTS} > Q_{H_2O_2} > Q_{bare,}$ yet it is further confirmed by the experimental measurements as depicted in Fig. 8a.

Fig. 9 shows the comparison of normalized flow rates, which is in termed of ml min^{-1} V^{-1} cm^{-2}, for the present EO pumps subject to different treated PAAMs. Interestingly, the normalized flow rate is rather independent of supplied voltage for all membranes. The maximum normalized flow is near 0.1 ml min^{-1} V^{-1} cm^{-2} for APS-coated PAAM. It shows an approximate three-fold increase in this normalized flow rate when compared to that of the bare PAAM. In summary of the forgoing results, it is concluded that a considerable increase of performance for EO pumps can be achieved via surface charge density enhancement by modification of PAAM surfaces even without using any buffer control method.

5. Conclusion

The present study investigates how the surface modification, such as H_2O_2-pretreated, APS-coated, and MPTS-coated PAAMs, on PAA membrane influences the EO pumping performance. The FTIR spectra and contact angle measurements confirm that both APS and MPTS are effectively immobilized onto PAAM surfaces, providing higher surface charges on PAAM for EO pump performance enhancement in DI water. The surface charged enhancement is supported by the current measurement of EO pump. From Eq. (9) in Section 2.2, the conduction current is proportional to the surface charges density, which in turns indicates that the associated orders of surface charge and zeta potential are $\sigma_{APS} > \sigma_{MPTS} > \sigma_{H_2O_2} > \sigma_{bare}$ and $\zeta_{APS} > \zeta_{MPTS} > \xi_{H_2O_2} > \zeta_{bare}$, respectively. In other words, the surface charge density of the PAAM has been increased through the H_2O_2-pretreated, the APS- or MPTS-coated process. Using this result along with and the relation between the maximum volume flow rates of the EO pumps and the zeta potential of PAAM, e.g., see Eq. (7), one can anticipate the maximum volume flow rates of the EO pumps with these four kinds of PAAMs are in the following order: $Q_{APS} > Q_{MPTS} > Q_{H_2O_2} > Q_{bare,}$. This conclusion can be confirmed by present flow rate measurements.

The characteristic of EO pumps with these four kinds PAAMs are compared. The ratios of the normalized flow rates for the EO pump with the APS-coated PAAM, the MPTS-coated PAAM, and the bare PAAM are approximately 3:2:1, respectively. Although the EO pump with APS-coated PAAM owns the highest flow rate; however, its lifetime is also the shortest. The EO pump with MPTS-coated PAAM shows not only higher flow rate but also exhibits durable operation throughout the experiments. The flow rates of the EO pumps with those coated-PAAMs are demonstrated to be enhanced without the need for any buffer control.

Acknowledgements

This work was supported by the Bureau of Energy and the Department of Industrial Technology, both under the Ministry of Economic Affairs, Taiwan, R.O.C.

References

[1] D.J. Laser, J.G. Santiago, A review of micropumps, J. Micromech. Microeng. 14 (2004) R35–R64.
[2] L. Jiang, J. Mikkelsen, J.M. Koo, D. Huber, S. Yao, L. Zhang, P. Zhou, J.G. Maveety, R. Prasher, J.G. Santiago, T.W. Kenny, K.E. Goodson, Closed-loop electroosmotic microchannel cooling system for VLSI circuits, IEEE Trans. Compon. Pack. Technol. 25 (2002) 347–355.
[3] R.B. Schoch, L.F. Cheow, J. Han, Electrical detection of fast reaction kinetics in nanochannels with an induced flow, Nano Lett. 7 (12) (2007) 3895–3900.
[4] S.L. Zeng, C.H. Chen, J.C. Mikkelsen, J.G. Santiago, Fabrication and characterization of electroosmotic micropumps, Sens. Actuators B 79 (2001) 107–114.
[5] D.S. Reichmuth, G.S. Chirica, B.J. Kirby, Increasing the performance of high-pressure, high-efficiency electrokinetic micropumps using zwitterionic solute additives, Sens. Actuators B 92 (2003) 37–43.
[6] P. Wang, Z. Chen, H.C. Chang, A new electro-osmotic pump based on silica monoliths, Sens. Actuators B 113 (2006) 500–509.
[7] S. Yao, A.M. Myers, J.D. Posner, K.A. Rose, J.G. Santiago, Electroosmosis pumps fabricated from porous silicon membranes, J. Microelectromech. Syst. 15 (3) (2006) 717–728.
[8] W. Chen, J.H. Yuan, X.U. Xia, Characteristic and manipulation of the electroosmotic flow in porous anodic alumina membranes, Anal. Chem. 77 (2005) 8102–8108.
[9] S.K. Vajandar, D. Xu, D.A. Markov, J.P. Wikswo, W. Hofmeister, D. Li, SiO_2-coated porous anodic alumina membranes for high flow rate electroosmosis pumping, Nanotechnology 18 (2007) 275705.
[10] Y.F. Chen, M.C. Li, Y.H. Hu, W.J. Chang, C.C. Wang, Low-voltage electroosmotic pumping using porous anodic alumina membranes, Microfluid. Nanofluid. 5 (2008) 235–244.
[11] J. Miao, M. Xu, X. Zhang, N. Wang, Z. Yang, P. Sheng, Micropumps based on the enhanced electroosmotic effect of aluminum oxide membranes, Adv. Mater. 19 (2007) 4234–4237.
[12] H.J. Modi, D.W. Fuerstenau, Streaming potential studies on corundum in aqueous solutions of inorganic electrolytes, J. Phys. Chem. 61 (1957) 640–643.
[13] R.J. Hunter, Zeta Potential in Colloid Science: Principles and Applications, Academic Press Inc., London, 1981.
[14] Z. Ma, Z. Mao, Z.C. Gao, Surface modification and property analysis of biomedical polymers used for tissue engineering, Colloids Surf. B: Biointerf. 60 (2) (2007) 137–157.
[15] S. Levine, J.R. Marriott, G. Neal, N. Epstein, Theory of electrokinetic flow in fine cylindrical capillaries at high zeta potential, J. Colloid Interf. Sci. 52 (1975) 136–149.
[16] D. Stein, M. Kruithof, C. Cekker, Surface-charge-governed ion transport in nanofluidic channels, Phys. Rev. Lett. 93 (3) (2004) 035901-1–035901-4.
[17] A. Carrè, V. Lacarrière, Study of surface charge properties of minerals and surface-modified substrates by wettability measurements, Contact Angle Wettab. Adhes. 4 (2006) 1–14.
[18] D. Son, A. Wolosiuk, P.V. Braun, Double direct templated hollow ZnS microspheres formed on chemically modified silica colloids, Chem. Mater. 21 (4) (2009) 628–634.
[19] R. Karnik, K. Castelino, R. Fan, P. Yang, A. Majumdar, Effects of biological reactions and modifications on conductance of nanofluidic channels, Nano Lett. 5 (9) (2005) 1638–1642.
[20] A.V. Krasnoslobodtsev, S.N. Smirnov, Effect of water on silanization of silica by trimethoxylsilanes, Langmuir 18 (2002) 3181–3184.
[21] C. Wu, T. Xu, W. Yang, A new inorganic–organic negatively charged membranes: membrane preparation and characterizations, J. Membr. Sci. 224 (2003) 117–125.
[22] D.G. Kurth, T. Bein, Quantification of the reactivity of 3-aminopropyltriethoxysilane monolayers with the quartz-crystal microbalance, Angew. Chem. Int. Ed. Engl. 31 (3) (1992) 336–338.
[23] J.F. Liu, L.G. Zhang, N. Gu, J.Y. Ren, Y.P. Wu, Z.H. Lu, P.S. Mao, D.Y. Chen, Fabrication of colloidal gold micro-patterns using photolithographed self-assembled monolayers as templates, Thin Solid Films 327–329 (1998) 176–179.
[24] L. Xu, J. Liao, L. Huang, N. Gu, H. Zhang, J. Liu, Pedant thiol groups-attached Pd(II) for initiating metal deposition, Appl. Surf. Sci. 211 (2003) 184–188.

[25] I. Rodríguez, N. Chandrasekhar, Experimental study and numerical estimation of current changes in electroosmotically pumped microfluidic devices, Electrophoresis 26 (2005) 1114–1121.
[26] S. Arulanandam, D. Li, Determining, ζ potential and surface conductance by monitoring the current in electro-osmotic flow, J. Colloid Interf. Sci. 225 (2000) 421–428.

Biographies

Yu-Feng Chen received her B.S. degree in Nuclear Engineering and the Ph.D. degree in Power Mechanical Engineering from National Tsing Hua University (NTHU), Taiwan, in 1994 and 2002, respectively, and M.S. degree in Aeronautics and Astronautics Engineering from National Cheng Kung University, Taiwan, in 1996. She is a researcher of the Energy & Environment Laboratories (EEL), Industrial Technology Research Institute (ITRI). Her interesting research fields include micro-flows and heat transfer, micro-pump, and supercapacitor.

Yi-Hsin Hu received his B.S. degree in 2006 and M.S. degree in 2008 both from Department of Chemical and Materials Engineering, National Yunlin University of Science and Technology in 2008. His master thesis is related to the present EO pumping work. He is now in the Army for his one-year compulsory military service.

Yen-I Chou received the B.S., M.S., and Ph.D. degrees from National Cheng Kung University (NCKU), Tainan, Taiwan, in 1999, 2001, and 2005, respectively, all in Chemical Engineering. He joined in the Energy & Environment Laboratories (EEL), Industrial Technology Research Institute (ITRI), as a scientific researcher. His researches presently focus on microcantilever sensing technology, functional self-assembly monolayer, solid-state microsensor design and fabrication, electroless plating and nanoparticle preparation.

Shih-Ming Lai is a professor of Department of Chemical and Materials Engineering, National Yunlin University of Science and Technology. He received his B.S. degree in 1978 from National Taiwan University, and received his M.S. degree in 1983 and Ph.D. degree in 1987 from Washington University in St. Louis, USA. His research interests include adsorption, chromatography, membrane separation, and sensing technologies.

Chi-Chuan Wang obtained his B.S., M.S., and Ph.D. all in Mechanical Engineering from National Chiao-Tung University, Hsinchu, Taiwan during 1978–1989. After earning his Ph.D. in 1989, he joined the Energy & Environment Research Laboratories (EEL), Industrial Technology Research Institute (ITRI), Hsinchu, Taiwan as a researcher and is currently a senior lead researcher in ITRI. His research areas include enhanced heat transfer, multiphase system, heat pump and micro- and nano-scale energy conversion.